Global Science and Technology Journal
Vol. 4. No. 1. September 2016 Issue. Pp. 32 – 42

Initial Permeability Spectra of $Mn_{0.20}Zn_{0.50}Cu_{0.30}Fe_2O_4$ Synthesized by Combustion Method

F. Alam*[1] and A. K. M. Akther Hossain[2]

Frequency dependence initial permeability spectra of $Mn_{0.20}Zn_{0.50}Cu_{0.30}Fe_2O_4$ synthesized by auto combustion method *have been investigated. The X-ray diffraction patterns of this composition indicated that the sample possesses single phase cubic spinel structure. Sintering temperature (T_s) significantly affect on densification, grain growth and initial permeability of the samples. The grain size (D), bulk density (ρ_B), initial permeability (μ'_i) increases with increase in sintering temperature. The average grain size varied from 53-97 µm.The initial permeability strongly depends on average grain size, density and intragranular porosity. The real part of initial permeability increases from 799 to ~1100. The ferrite sample with higher initial permeability has a relatively lower resonance frequency obeying the Snoek's relation.*

Keywords: Initial permeability, Sintering temperature, Bulk density, Grain size.

1. Introduction

Magnetic materials are found in numerous products around us- home appliances, electronic products, automobiles, communications and data processing devices and equipments. These materials have now become a vital part of our everyday life in modern industries. Polycrystalline spinel ferrites, due to their excellent magnetic and physical properties are technologically very important. Ferrites are used in power electronics devices from radio frequency to microwave frequency, bubble devices, audio, video and digital recording, multi layer chip inductor and as permanent magnets. Substituted Mn-Zn ferrites are pertinent magnetic materials due to their high permeability, high magnetization, relatively high Néel temperature, low losses, low cost and environmental stability. These ferrites have been widely used in electrical and magnetic devices for high frequency applications (Praveena et al. 2009; Mathur et al. 2008; Kalarus et al. 2012; Goldman, 1990). The structural and magnetic properties of these ferrites can remarkably be controlled by the preparation condition, chemical composition, and sintering temperature. The main objective of the present research is to synthesize Cu substituted Mn-Zn ferrites having high permeability and low loss. To the best of our knowledge no work has been reported on $Mn_{0.20}Zn_{0.50}Cu_{0.30}Fe_2O_4$ and we are going to study its structural, physical and magnetic properties. Hossain and Rahman (2011) reported that the poor densification, slow grain growth rate can be remarkably improved and consequently initial permeability can be enhanced by the preparation condition and sintering temperature.

[1*]F. Alam, Corresponding Author, Department of Physical Sciences, School of Engineering and Computer Science, Independent University, Bangladesh (IUB), Dhaka, Bangladesh, Email: farhadiub@gmail.com
[2]A. K. M. Akther Hossain, Department of Physics, Bangladesh University of Engineering and Technology (BUET), Dhaka, Bangladesh, Email: akmahossain@phy.buet.ac.bd

The authors found a maximum initial permeability of 390, but in the present investigation we found a maximum initial permeability of 1061 which is remarkably higher than previous one. This paper is organized as follows: section 2 focuses on the literature review closely related to the present study. Section 3 describes sample preparation method and various characterization techniques. Section 4 explains the results and possible reasons behind these. Finally, section 5 presents our conclusions.

2. Literature Review

Several investigations on the properties of Ni-Mn-Zn (Singh et al. 2004), Ni-Cu-Zn (Su et al. 2004), Mg-Cu-Zn (Haque et al. 2008), Co-Mn-Zn Khan and Hossain (2012) ferrites have been reported. Ni and Lwin (2008) fabricated Mn-Zn ferrites at different sintering temperatures. From their observations, it is indicated that with increasing sintering temperature, grain growth increases and the average grain size increases and that grain growth leads to high permeability, small coercive field, small remanence, small hysteresis loop, rapid response to high-frequency magnetic fields in Mn-Zn ferrite. Pannaparayil et al. (1991) investigated the magnetic properties of high density Mn-Zn ferrites. High densities have been obtained upon sintering these ferrite powders at relatively low temperatures. It is seen that μ_i increases with increase in density. This is attributed to the variation in grain sizes of the ferrites with temperatures. Mn-Zn ferrites are extensively used in broad band and pulse transformer and wideband read heads for high definition video recording. For use in such devices, μ_i should remain constant over certain frequency ranges. Here in this case μ_i remains level at first, and then rises to a very shallow maximum before falling rapidly to a relatively low value due to ferromagnetic resonance. It was found that the larger the dc value of the permeability, the lower the frequency at which μ_i begins to drop. Hossain and Rahman (2011) studied on Cu substituted Ni-Zn ferrites on enhancement on microstructure and initial permeability. They found that Cu facilitates the grain growth and enhances the initial permeability with increase in sintering temperatures. As per our literature survey no work has been reported on $Mn_{0.20}Zn_{0.50}Cu_{0.30}Fe_2O_4$. Therefore it is fascinating to discuss the frequency dependence of initial permeability of $Mn_{0.20}Zn_{0.50}Cu_{0.30}Fe_2O_4$ at different sintering temperatures along with loss and quality factors of the sample.

3. Experimental Details

The ferrite powder of $Mn_{0.20}Zn_{0.50}Cu_{0.30}Fe_2O_4$ was synthesized by widely used auto combustion method which has the advantages of being fast, simple, short preparation duration and low energy consumption. The stoichiometric amounts of commercially available analytical grade powders of $MnCl_2.4H_2O$, $Cu(NO_3)_2.3H_2O$,$Zn(NO_3)_2.6H_2O$and Fe $(NO_3)_3.9H_2O$ were dissolved in ethanol to obtain a mixed homogenous solution. Ammonia solution was slowly added to metal nitrate solution to adjust the pH at 7. The solution was placed at constant temperature bath (~70ºC) followed by an ignition and formed a fluffy loose powders of the desired composition. The resultant powders of the samples were calcined at 700ºC for five hours in air. The grounded fine powders were then pressed into disk- and toroid-shaped samples. The samples prepared from each composition were sintered at 1200, 1250 and 1300ºC for five hours in air. During sintering, temperature ramps were 10ºC /min for heating and 5ºC /min for cooling. The structural characterization was carried out with an X-ray diffractometer using CuK_α radiation (λ = 1.54178Å). The lattice parameter for each composition was determined using Nelson-Riley function (Nelson & Riley 1945). The bulk density, ρ_B , of the samples

was determined using the expression $\rho_B = (W \times \rho)/W - W'$ where W and W' are the weight of the sample in air and water, respectively and ρ is the density of water at room temperature. The theoretical density, ρ_{th}, was calculated using the relation: $\rho_{th} = (ZM/N_A a^3)$, where N_A is Avogadro's number, M is the molecular weight of the corresponding composition, a^3 is the volume of the cubic unit cell and Z is the number of molecules per unit cell, which is 8 for the spinel cubic structure. The percentage porosity, P% was calculated from the relation $P(\%) = \{(\rho_{th} - \rho_B)/\rho_{th}\} \times 100$. The frequency dependent initial permeability was investigated using Wayne Kerr Impedance Analyzer (Model No.6500B). The complex permeability measurements on toroid- shaped samples were carried out at room temperature in the frequency range 100Hz-120MHz. The real part (μ_i') and the imaginary part (μ_i'') of the complex permeability were calculated using the following relations $\mu_i' = L_s/L_o$, and $\mu_i'' = \mu_i' \tan\delta$, where L_s is the self inductance of the sample core and $L_o = (\mu_o N^2 h/2\pi)\ln(r_o/r_i)$, is derived geometrically. L_o is the inductance of the winding coil without the sample core, N is the number of turns of the coil (N = 4), h is the thickness, r_o is the outer radius and r_i is the inner radius of the toroid shaped sample. The relative quality factor, Q was calculated from the relation: $Q = \mu_i'/\tan\delta$, where tanδ is the loss factor.

4. Results and Discussion

4.1 Lattice Parameter, Density and Porosity

Fig.1 shows the typical X-ray diffraction pattern of $Mn_{0.20}Zn_{0.50}Cu_{0.30}Fe_2O_4$ sintered at 1250ºC. The observed diffraction lines indicate that the sample is of cubic spinel structure without any unreacted constituent present in the sample. The lattice parameter was determined by using the Nelson-Riley extrapolation method. The lattice parameters obtained were plotted against Nelson-Riley function $F(\theta) = 1/2\left[\cos^2\theta/\sin\theta + \cos^2\theta/\theta\right]$, where θ, the Bragg's angle and straight lines are obtained (Nelson & Riley 1945). The exact values of lattice constant were estimated from the extrapolation of these lines to $F(\theta) = 0$ or $\theta = 90°$. The lattice constant was obtained 8.4212Å. Density plays an important role in controlling the properties of polycrystalline ferrites. Fig. 2 shows the presence of Cu on bulk density in $Mn_{0.20}Zn_{0.50}Cu_{0.30}Fe_2O_4$ ferrite sintered at various temperatures. It is found that bulk density increases with increase sintering temperatures while the porosity follows the opposite trend. The increase in bulk density can be attributed to the difference in atomic weight and specific gravity of the ferrites components. The atomic weight and density of Cu^{2+} (63.55 amu and 8.94g.cm^{-3}) is greater than that of Mn^{2+} (55.94 amu and 7.21g.cm^{-3}) (Williams 1996). The effect of addition of Cu on the microstructure has been reported by Haque et al. (2008), who found that Cu ion accelerates the grain growth and also favour densification. These combined factors contributed to the reduction of porosity, which consequently enhanced the density of the ferrite reported by Shirsath et al. (2010). This is because during the sintering process, the thermal energy generates a force that drives the grain boundaries to grow over pores, thereby decreasing the pore volume and increases the density of the material. Our obtained result agrees well with the reported value by Haque et al. (2008).The increase in bulk density can be related with the lattice constant, since the molecular weight increases which overtake the increase in volume of the unit cell and hence density increases with increase in Cu content. The increase in density and

decrease in percentage porosity (P %) of $Mn_{0.20}Zn_{0.50}Cu_{0.30}Fe_2O_4$ for different sintering temperatures are tabulated in Table 1.

Figure 1: The X-Ray Diffraction Pattern of $Mn_{0.20}Zn_{0.50}Cu_{0.30}Fe_2O_4$ Sintered at 1250 °C in Air

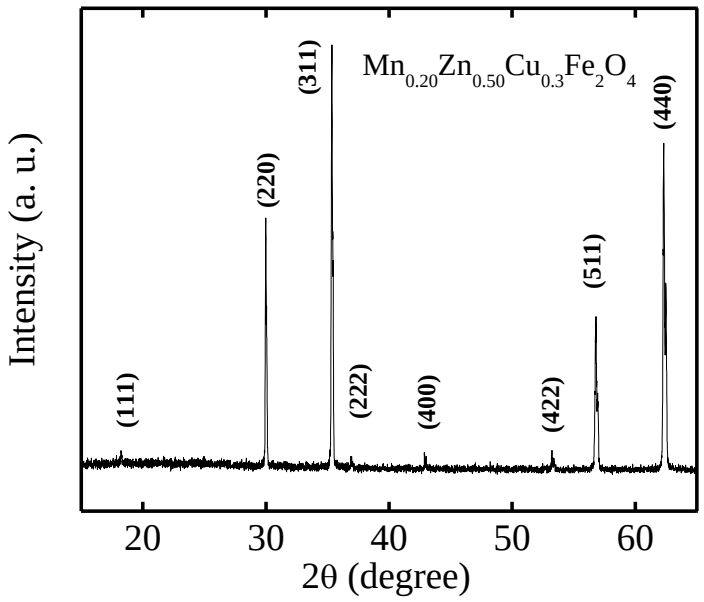

Figure 2: The Variation of Density and Porosity for $Mn_{0.20}Zn_{0.50}Cu_{0.30}Fe_2O_4$ Sintered at Different Temperatures

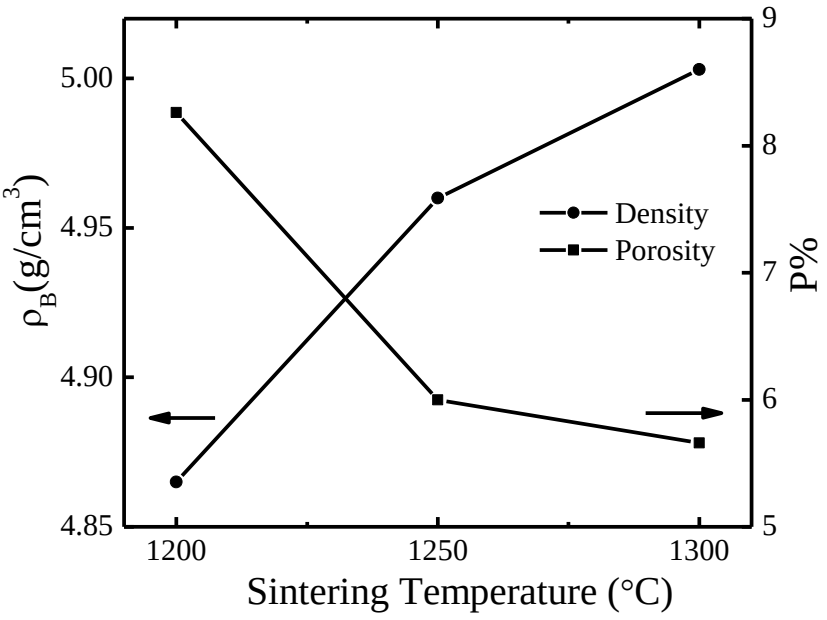

4.2 Microstructures

The surface morphology of $Mn_{0.20}Zn_{0.50}Cu_{0.30}Fe_2O_4$ ferrite sample is observed by high resolution optical micrograph (Olympus DP-70) for determining the average grain size of the samples. Grain size is an important parameter affecting the magnetic properties of ferrites. The micrographs shown in Fig. 3 reveal that the grain size is influenced by the copper in the composition and also on the sintering temperatures. The average grain sizes vary from 53 to 97 μm. The grain size increases with increase in sintering temperature can be reasonably explained on the basis of sintering mechanism. Cu influences the microstructure by the formation of liquid phase during sintering. It facilitates the grain growth which can be attributed to the fact that Cu increases the rate of cation interdiffusion as a result of segregation to the grain boundaries as observed by Low and Sale (2002). The behavior of grain growth reflects the competition between the driving force for grain boundary movement and the retarding force exerted by pores (Low & Sale 2002). When the driving force of the grain boundary in each grain is homogeneous, the sintered body attains a uniform grain size distribution. Average grain sizes of the samples are determined by linear intercept technique (Mendelson 1969) and are presented in the Table 1. Effects of sintering temperature on grain growth of $Mn_{0.20}Zn_{0.50}Cu_{0.30}Fe_2O_4$ ferrite has been investigated and is shown in Fig. 3. The average grain size increases with increasing sintering temperatures. This is because during the sintering process, the thermal energy generates a force that drives the grain boundaries to grow over pores, thereby decreasing the pore volume and increasing the grain sizes.

Figure 3: Optical Micrographs of $Mn_{0.20}Zn_{0.50}Cu_{0.30}Fe_2O_4$ Sintered at Different Sintering Temperatures

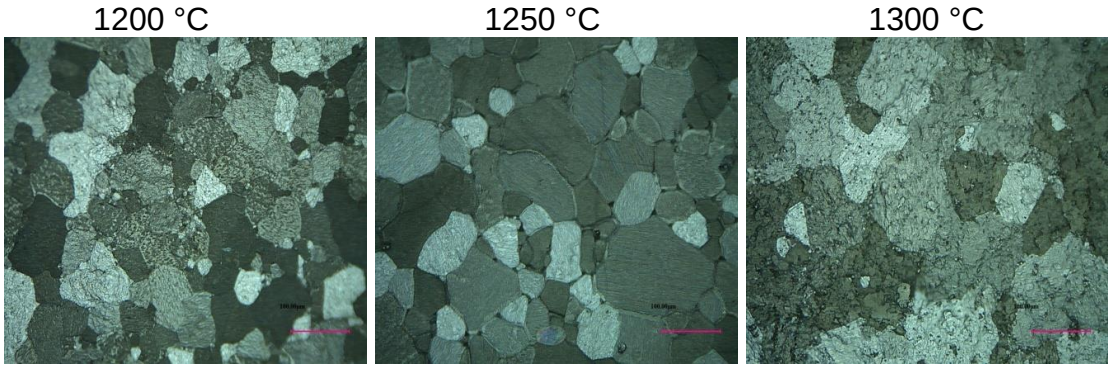

4.3 Frequency Dependence of Complex Permeability

Fig. 4 shows the initial permeability spectra as a function of frequency for $Mn_{0.20}Zn_{0.50}Cu_{0.30}Fe_2O_4$ ferrite sintered at 1200, 1250 and 1300ºC. The complex permeability is given by $\mu^* = \mu_i' - i\mu_i''$, where μ_i' and μ_i'' are the real and imaginary parts of complex permeability, respectively. μ_i' describes the stored energy expressing the component of magnetic induction B in phase and μ_i'' describes the dissipation of energy expressing the component of B 90° out of phase with the alternating magnetic field H. From Fig.4, it is seen that μ_i' remains almost flat until the frequency is raised to a certain level and then drops fairly to very low at higher frequencies. μ_i'' gradually decreases with frequency and took a broad maximum at a certain frequency, where μ_i' rapidly decreases as shown in Fig. 5. The frequency at which μ_i' attain the highest value is known as the resonance frequency, f_r. The f_r is the utility range of frequency of a

magnetic material up to which the material can be used efficiently. At the resonance, maximum energy is transferred from the applied field to the lattice resulting in the rapid increase in loss factor (tanδ) as shown in Fig. 6. It is also observed from Fig. 4 that the higher the permeability of the specimen, the lower the frequency of the resonance (Snoek 1948).The values of μ_i' at a constant frequency of 100Hz for $Mn_{0.20}Zn_{0.50}Cu_{0.30}Fe_2O_4$ sintered at various temperatures are presented in Table 1. It is well known that the permeability of polycrystalline ferrite is related to two magnetizing mechanism: domain wall motion and spin rotation. The domain walls normally remain pinned to the grain boundary and bulged when subjected to any small magnetic as described by Globus et al. (1971). It was assumed that the permeability due to the wall motion is likely to be linearly dependent on the grain size, while the permeability contribution due to spin rotation was assumed to be independent of grain size. Globus et al. (1971) studied several Ni-Zn ferrites and found a linear relationship between permeability and grain size (D). Kakaktar et al. (1996) studied the effect of grain size on μ_i' and found that $\mu_i' \propto D$. Perduijin and Peloschek (1968) and Peloschek and Perduijin (1968) also found a linear relation between μ_i' and grain size in Mn-Zn ferrite. The permeability due to domain wall motion can be expressed by Globus-Duplex relation $\mu_i' \propto \left(M_S^2 D / \sqrt{K_1}\right)$, where M_S is the saturation magnetization; K_1 is the anisotropy constant (Globus et al. 1971). Thus the domain wall motion is greatly affected by the average grain size. This is because bigger grains tend to contain large number of domain walls and μ_i' being a result of the easy reversal of domain wall displacement in the direction of the applied magnetic field. As the number of walls increases with the grain sizes, the contribution of wall movement to magnetization is increased. In our present study of microstructure, it is seen that the grain size increases significantly with increase in sintering temperature. Therefore the increase of μ_i' with increasing sintering temperature is justified. Fig. 7 shows the variation of permeability at different frequencies of $Mn_{0.20}Zn_{0.50}Cu_{0.20}Fe_2O_4$ sintered at different sintering temperatures. There is a decreasing trend in permeability with increase in frequency. This is because at higher frequencies nonmagnetic impurities between grains and intragranular pores act as pinning points and increasingly hinders the motion of spin and domain walls thereby decreasing their contribution to permeability and also increasing the loss (Hossain and Rahman 2011; Globus et al. 1971). It is observe from Fig. 8 that μ_i' increases with increase in sintering temperature T_s and density. This increase in μ_i' with increasing T_s is attributed to the contribution of domain wall motion, which becomes more significant as the sintered density and grain size increases. Generally, a higher μ_i' is obtained through the control of both the composition and microstructure which depends on sintering conditions. The frequency of relative quality factor of the samples sintered at various temperatures was calculated from the magnetic loss tangent. For practical application the quality factor is often used as a measure of performance. The RQF increases with an increase of frequency, showing a peak and then decreases with further increase in frequency as seen from Fig. 9. The variation of RQF with frequency is observed that the sample sintered at 1250°C has the highest RQF (5420). The highest RQF for $Mn_{0.20}Zn_{0.50}Cu_{0.30}Fe_2O_4$ is 5420, probably due to the growth of less imperfection and defects compared to those of other samples (Hossain and Rahman 2011).

Figure 4: The Variation Real Part of Initial Permeability of $Mn_{0.20}Zn_{0.50}Cu_{0.30}Fe_2O_4$ Sintered at Different Temperatures

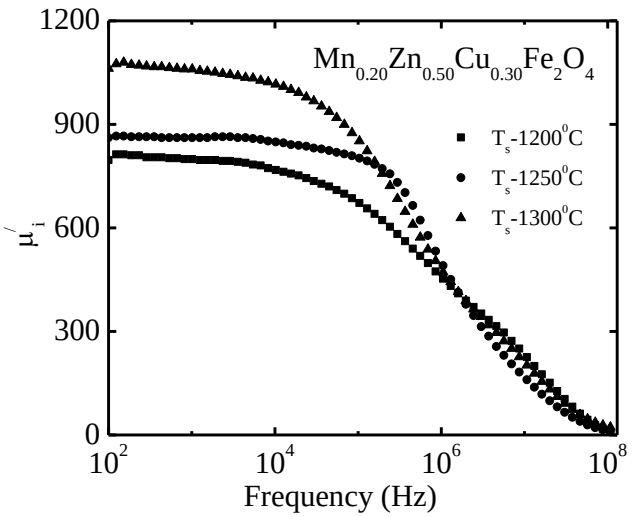

Figure 5: The Variation of Imaginary Part of Initial Permeability of $Mn_{0.20}Zn_{0.50}Cu_{0.30}Fe_2O_4$ Sintered at Different Temperatures

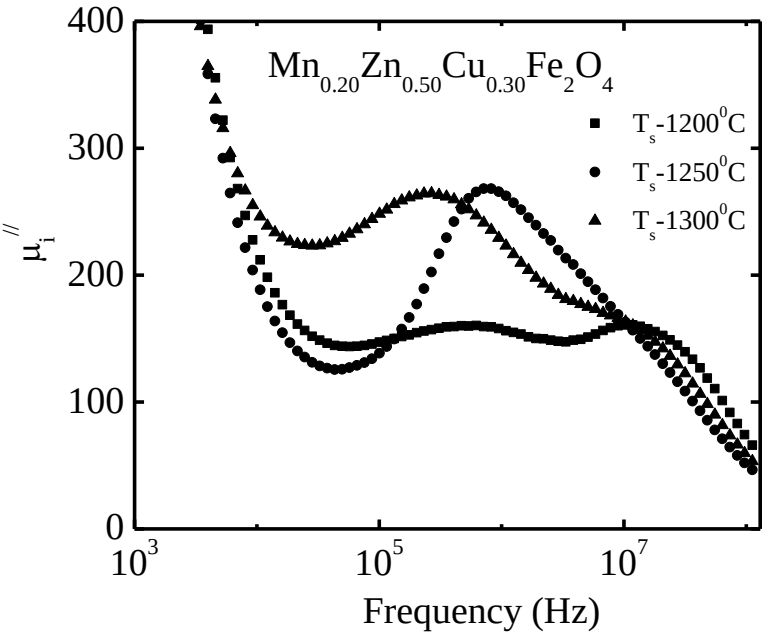

Figure 6: The Variation of Loss Factor of $Mn_{0.20}Zn_{0.50}Cu_{0.30}Fe_2O_4$ Sintered at Different Temperatures.

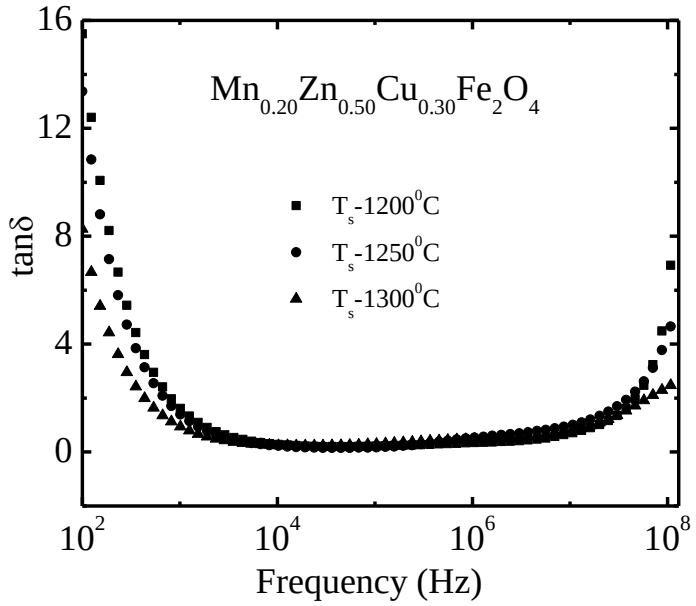

Figure 7: The Variation Real Part of Initial Permeability of $Mn_{0.20}Zn_{0.50}Cu_{0.30}Fe_2O_4$ at Different Frequencies, Samples Sintered at Different Temperatures

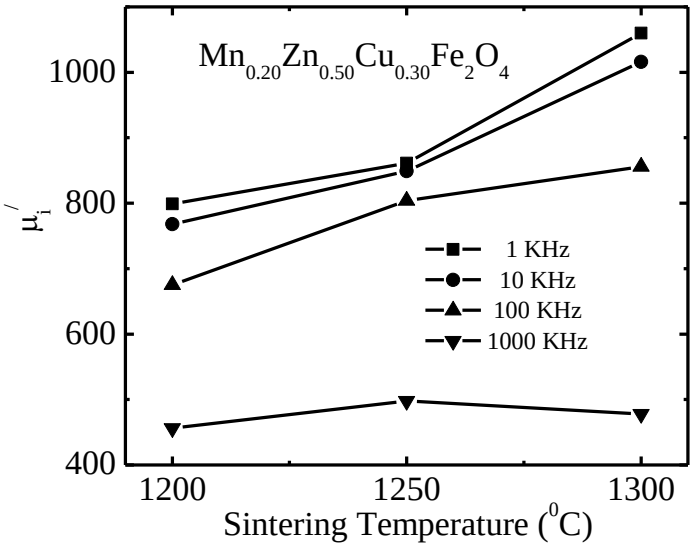

Figure 8: The Variation Real Part of Initial Permeability and Density of $Mn_{0.20}Zn_{0.50}Cu_{0.30}Fe_2O_4$ Samples Sintered at Different Temperatures

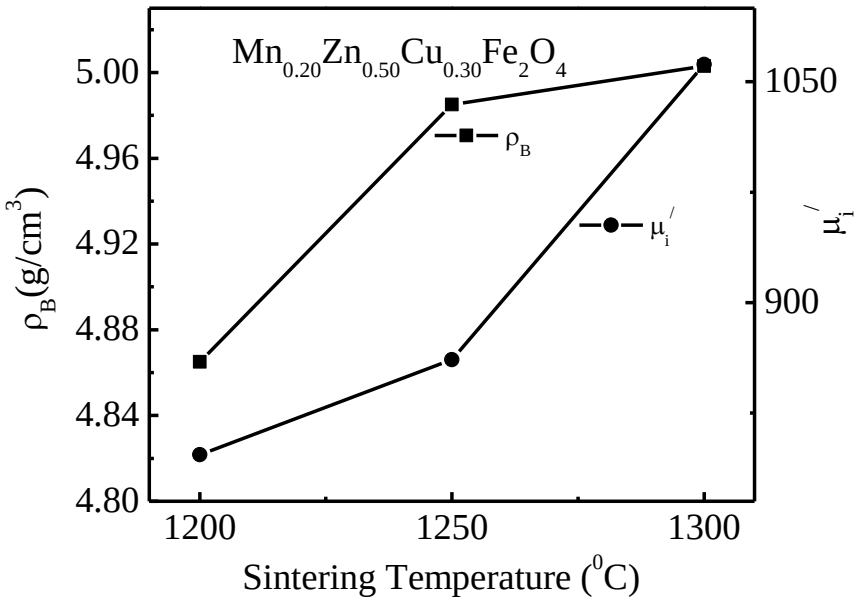

Table 1: Lattice Constant, Density, Porosity, Average Grain Size, Initial Permeability and Relative Quality Factor of $Mn_{0.20}Zn_{0.50}Cu_{0.30}Fe_2O_4$

T_s (°C)	a (Å)	ρ_{th} (gm/ cm^3)	ρ_B (gm/ cm^3)	P (%)	D (μm)	μ_i' (at 100Hz)	Q_{max}
1200			4.865	8.26	52.6	796	3621
1250	8.4212	5.3033	4.960	6.00	56.0	861	5423
1300			5.003	5.66	97.0	1061	4352

Figure 9: The Variation Relative Quality Factor of $Mn_{0.20}Zn_{0.50}Cu_{0.30}Fe_2O_4$ Sintered at Different Temperatures

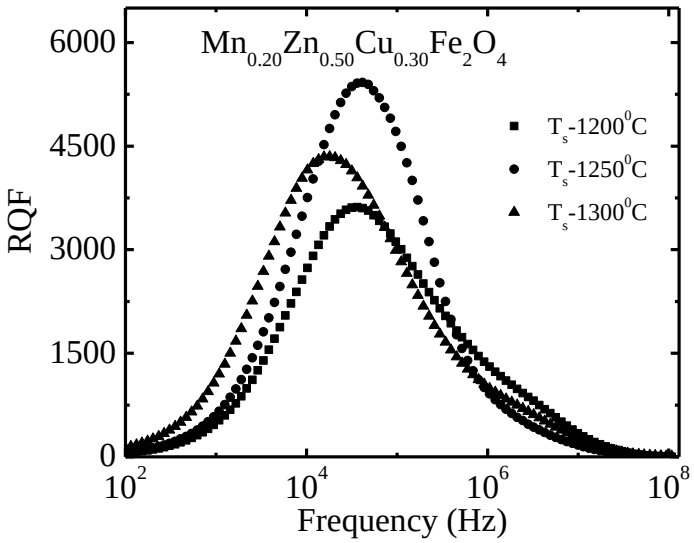

5. Conclusions

The ferrite sample prepared by auto combustion method is of single phase cubic spinel structure that has been confirmed from X-ray diffraction pattern. The bulk density and average grain size increase with increase in sintering temperatures. The high density material can be obtained through auto combustion method due to the formation of homogeneous solution in this method. Initial permeability increases with increase in sintering temperature which is attributed to the increased density and average grain size of the sample. The optimum initial permeability in the present case is much higher than reported by Hossain as mentioned in section 1. The highest RQF (5420) was obtained for the sample sintered at 1250 °C. Initial permeability is remarkably enhanced and these ferrites could be important and suitable for technological applications. Further studies on different characteristics are possible for fundamental interest of the studied sample. Magnetic field dependent magnetization can be carried out to determine various magnetic parameters such as saturation magnetization, remanent magnetization, coercivity etc. Neutron diffraction analysis may be performed for these compositions to determine the distribution of ions between A- and B- sites.

References

Globus, A, Duplex, P and Guyot, M 1971, 'Determination of initial magnetization curve from crystallites size and effective anisotropy field', IEEE Transactions on Magnetics, vol. 7, no. 3, pp. 617-622.

Goldman, A 1990, 'Modern Ferrite Technology', Van Nostrand Reinhold, New York.

Haque, MM, Huq, M and Hakim, MA 2008, 'Influence of CuO and sintering temperature on the microstructure and magnetic properties of Mg-Cu-Zn ferrites', Journal of Magnetism and Magnetic Materials, vol. 320, no. 21, pp. 2792-2799.

Hossain, AKMA, Rahman, ML 2011, 'Enhancement of microstructure and initial permeability due to Cu substitution in $Ni_{0.50-x}Cu_xZn_{0.50}Fe_2O_4$ ferrites', Journal of Magnetism and Magnetic Materials, vol. 323, no. 15, pp. 1954-1962.

Kakatkar, SV, Kakatkar, SS, Patil, RS, Sankpal, AM, Chaudhari, ND, Maskar, PK, Sawant, SR 1996, 'Effect of sintering conditions and Al^{3+} addition on wall permeability in $Ni_{1-x}Zn_xAl_tFe_{2-t}O_4$ ferrites. Materials Chemistry and Physics, vol. 46, no. 1, pp. 96-99.

Kalarus, J, Kogias, G, Holz, D and Zaspalis, VT 2012, 'High permeability-high frequency stable MnZn ferrites', Journal of Magnetism and Magnetic Materials, vol. 324, no. 18, pp. 2788-2794.

Khan, MHR, Hossain, AKMA 2012, 'Reentrant spin glass behavior and large initial permeability of $Co_{0.5-x}Mn_xZn_{0.5}Fe_2O_4$', Journal of Magnetism and Magnetic Materials, vol. 324, no. 4, pp. 550-558.

Low, KO & Sale, FR 2002, 'Electromagnetic properties of gel-derived NiCuZn ferrites', Journal of Magnetism and Magnetic Materials, vol. 246, no. 1-2, pp. 30-35.

Mendelson, MI 1969, 'Average grain size in polycrystalline ceramics', Journal of American Ceramic Society, vol. 52, no. 8, pp. 443-446.

Nelson, JB and Riley, DP 1945, 'An experimental investigation of extrapolation methods in derivation of accurate unit-cell dimensions of crystals', Proceedings of the Physical Society, vol. 57, no. 3, pp. 160-177.

Ni, SM and Lwin, KT 2008, 'Production of Manganese-Zinc Ferrite Cores for Electronic Applications, World Academy of Science, Engineering and Technology, vol. 2, pp. 130-135.

Pannaparayil, T, Marande, R, and Komarneni, S 1991, 'Magnetic properties of high-density Mn-Zn ferrites', Journal of Applied Physics, vol. 69, no. 8, pp. 5349-5351.

Peloschek, H and Perduijn, D 1968, 'High-permeability MnZn ferrites with flat μ-T curves', IEEE Transactions on Magnetics, vol. 4, no. 3, pp. 453–455.

Perduijn, DJ and Peloschek, HP 1968, 'Mn-Zn ferrites with very high frequency', Proceedings of the British Ceramic Society, vol. 10, pp. 263-273.

Praveena, K, Sadhana, K, Bharadwaj, S and Murthy, SR 2009, 'Developement of nanocrystalline Mn-Zn ferrites for high frequency transformer applications', Journal of Magnetism and Magnetic Materials, vol. 321, no. 16, pp. 2433-2437.

Shirsath, SE, Toksha, BG, Kadam, RH, Patage, SM, Mane, DR, Jangam, GS and Ghashemi, A 2010, 'Doping effect of Mn2+on the magnetic behavior in Ni-Zn ferrite nanoparticles prepared by sol-gel auto-combustion', Journal of Physics and Chemistry of Solids, vol. 71, no. 12, pp. 1669-1675.

Singh, AK, Singh, AK, Goel, TC and Mendiratta, RG 2004, 'High performance Ni-substituted Mn-Zn ferrites processed by soft chemical technique', Journal of Magnetism and Magnetic Materials, vol. 281, no. 2-3, pp. 276-280.

Snoek, JL 1948, 'Dispersion and absorption in magnetic ferrites at frequencies above one Mc/s', Physica, vol. XIV, no. 4, pp. 207-217.

Su, H, Zhang, H, Tang, X and Xiang, X 2004, 'High-permeability and high-Curie temperature NiCuZn ferrite', Journal of Magnetism and Magnetic Materials, vol. 283, no. 2-3, pp. 157-163.

Williams, ML 1996, *CRC* Handbook of Chemistry and Physics, 76th edition. Occupational and Environmental Medicine, vol. 53, no. 7, pp. 504–504.